European Journal of Medicinal Chemistry 44 (2009) 4353–4361

Contents lists available at ScienceDirect

European Journal of Medicinal Chemistry

journal homepage: http://www.elsevier.com/locate/ejmech

Original article

Metals in anticancer therapy: Copper(II) complexes as inhibitors of the 20S proteasome

Sarmad Sahiel Hindo [a], Michael Frezza [b], Dajena Tomco [a], Mary Jane Heeg [a], Lew Hryhorczuk [a], Bruce R. McGarvey [c], Q. Ping Dou [b,**], Cláudio N. Verani [a,*]

[a] Department of Chemistry, Wayne State University, Detroit, MI 48202, USA
[b] The Prevention Program, Barbara Ann Karmanos Cancer Institute and Department of Pathology, School of Medicine, Wayne State University, Detroit, MI 48201, USA
[c] Department of Chemistry and Biochemistry, University of Windsor, Windsor, ON N9B 1P4, Canada

ARTICLE INFO

Article history:
Received 3 April 2009
Received in revised form
19 May 2009
Accepted 20 May 2009
Available online 24 May 2009

Keywords:
Proteasome inhibition
Anticancer therapy
Copper(II)
Metallodrugs
Bioinorganic

ABSTRACT

Selective 20S proteasomal inhibition and apoptosis induction were observed when several lines of cancer cells were treated with a series of copper complexes described as [Cu(L^I)Cl] (**1**), [Cu(L^I)OAc] (**2**), and [Cu(HL^I)(L^I)]OAc (**3**), where HL^I is the ligand 2,4-diiodo-6-((pyridine-2-ylmethylamino)methyl)phenol. These complexes were synthesized, characterized by means of ESI spectrometry, infrared, UV–visible and EPR spectroscopies, and X-ray diffraction when possible. After full characterization species **1**–**3** were evaluated for their ability to function as proteasome inhibitors and apoptosis inducers in C4-2B and PC-3 human prostate cancer cells and MCF-10A normal cells. With distinct stoichiometries and protonation states, this series suggests the assignment of species $[CuL^I]^+$ as the minimal pharmacophore needed for proteasomal chymotryspin-like activity inhibition and permits some initial inference of mechanistic information.

1. Introduction

The investigation of metal-based complexes in anticancer drug discovery has been precipitated by the clinical effectiveness [1] and understanding of the mechanisms [2] of platinum-containing drugs. Nonetheless, toxicity and acquired drug resistance have been hampering the widespread use of such metallodrugs [3]. These findings have fostered efforts toward the rational development of metal-containing agents that present modes of action distinct from those of cisplatin and its derivatives [4].

A modern target in cancer treatment, the 26S proteasome is a large multicatalytic protease complex composed of two terminal 19S regulatory caps and a 20S proteolytic core [5]. This complex is responsible for the degradation of many endogenous proteins including misfolded or damaged proteins to ensure normal cellular function [6]. The ubiquitin–proteasome pathway plays an essential role in multiple cellular processes, including cell cycle progression, apoptosis, differentiation and senescence. It has been shown that human cancer cells are more sensitive to proteasome inhibition than normal cells, indicating that proteasome inhibitors could be used as novel anticancer drugs [7]. Therefore, inhibition of the 20S core particle in the 26S proteasome by substrate modifications such as alkylations, and ring formations has been demonstrated by a number of organic species such as lactacystin [8], macrocyclic esters [9], epoxyketones [10], and several peptide derivatives [11], including recently FDA-approved boronates [12,13]. The premise that stoichiometric mixtures of copper ions with organic chelators can form a new class of proteasome inhibitors has been investigated by the Dou Group in recent years [14,15]. Similarly, discrete gallium complexes with the asymmetric $N_{pyridine}N'_{amine}O_{phenolate}$ 2,4-di-X-6-((pyridine-2-ylmethylamino)methyl)phenol ligands HL^X (where X = H, *tert*-butyl, bromo, or iodo) were synthesized by the Verani Group. The bromo or iodo-substituted species rendered effective against cisplatin-resistant neuroblastoma [16], as well as for a number of other tumors [17]. The link between the *in vitro* and *in vivo* activities of these gallium complexes and proteasome inhibition has been established recently in a joint article [18]. In the course of this work, we observed that *in situ* complexation of HL^{Br}

* Correspondence to: Cláudio N. Verani, Department of Chemistry, Wayne State University, 5101 Cass Ave, Detroit, MI 48202, USA. Tel.: +1 313 577 1076; fax: +1 313 577 8022.
** Corresponding author. The Prevention Program Barbara Ann Karmanos Cancer Institute, Department of Pathology, School of Medicine, Wayne State University, 4100 John R Road, Detroit, MI 48201, USA. Tel.: +1 313 576 8301; fax: +1 313 576 8307.
E-mail addresses: doup@karmanos.org (Q.P. Dou), cnverani@chem.wayne.edu (C.N. Verani).

0223-5234/$ – see front matter © 2009 Elsevier Masson SAS. All rights reserved.
doi:10.1016/j.ejmech.2009.05.019

or HL^I with bivalent transition metal salts leads to the generation of species that display superior performance in cell death assays when compared to the equivalent gallium species.

Because detailed knowledge of the nature of the pharmacophore is pivotal to the understanding of the underlying mechanisms for metal-based proteasome inhibition, we present in this article a thorough study that encompasses the synthesis, spectrometric and spectroscopic characterization, and pharmacological evaluation of a series of copper complexes with the ligand HL^I. The systems investigated in this article are $[Cu(L^I)Cl]$ (**1**), $[Cu(L^I)OAc]$ (**2**), and $[Cu(HL^I)(L^I)]OAc$ (**3**), as displayed in Scheme 1. These copper complexes were found to be able to induce proteasomal inhibition and apoptosis in cultured human prostate cancer and leukemia cells. Based on these results, we conclude with suggestions for some initial mechanistic insights on how these complexes may act. The findings described in this paper might have an impact in the development of a novel route to cancer therapy.

2. Results and discussion

2.1. Ligand design and in situ copper complexation

The iodo-substituted ligand 2,4-diiodo-6-((pyridine-2-ylmethylamino)methyl)phenol, HL^I was synthesized by treatment of 2-hydroxy-3,5-diiodobenzaldehyde with 2-aminomethylpyridine followed by reduction with sodium borohydride [16]. It can be considered as an evolution from its terbutylated analogues inspired by biomimetic efforts to model redox-active enzymes such as galactose-oxidase [19]. The complexes were designed considering that a metal ion coordinated to the ligand could bind to the 20S core of the proteasome, possibly *via* the terminal threonine residue Thr1 or another available coordination site. Initial exploratory studies on human C4-2B prostate cancer cells comprised of cell death induced by a stoichiometric mixture of HL^I and copper(II) chloride in DMSO and toward proteasomal activity in whole-cell extracts. These assays showed that the resulting HL^I:$CuCl_2$:DMSO mixture was fourfold more potent than the recently reported gallium species.

2.2. Syntheses, spectrometry, and spectroscopic characterization of *1*–*3*

Spectrometric evaluation of the stoichiometric HL^I:$CuCl_2$:DMSO mixture using ESI in the positive mode led to the identification of monomeric and dimeric fragments that may act as pharmacophores to the inhibition of the proteasome complex. These fragments fit well with the expected distribution anticipated in systems containing copper and iodine isotopes. The relative ESI-MS profile for the monomeric $[CuL^I]^+$ with an $m/z = 527.9$ is shown in Fig. 1.

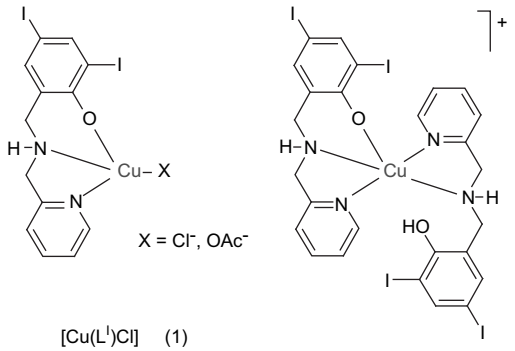

$[Cu(L^I)Cl]$ (1)

$[Cu(L^I)OAc]$ (2)

$[Cu(HL^I)(L^I)]OAc$ (3)

Scheme 1. Copper(II) complexes.

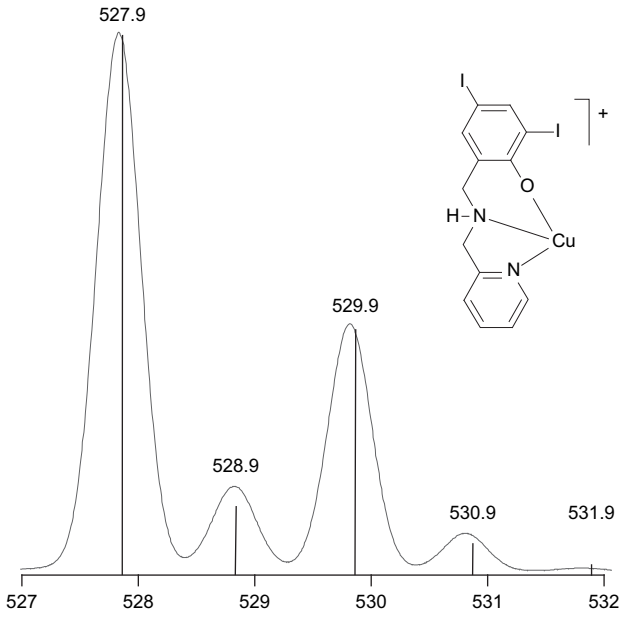

Fig. 1. Experimental (bars) and simulated (continuum) ESI MS m/z data for monomeric $[CuL^I]^+$.

A minor peak at $m/z = 994$ is also detectable in this mixture suggesting a 2:1 ligand-to-copper complex, where either two fully deprotonated ligands are coordinated to the metal ion as in $\{[Cu(L^I)_2] + H^+\}^+$ or one of the ligands remains protonated as in $[Cu(HL^I)(L^I)]^+$, respecting a 5-coordination preference imposed by the Jahn–Teller effect expected by a $3d^9$ species such as the copper(II) ion. Based on similar systems [20], the latter proposition is favored.

With the intent of isolating and testing these species as anticancer agents, reactions with 1:1, and 2:1 ligand-to-metal ratios were performed. Treatment of 1 equiv. of the ligand with 1 equiv. of $CuCl_2 \cdot 2H_2O$ in DMSO yielded a green solution that was precipitated with ethanol in 30% yield as a crystalline material.

The isolated product was characterized as $[Cu(L^I)Cl]$ (**1**). It is noteworthy that **1** can also be obtained using methanol or ethanol as solvents, and the choice of DMSO was intended to match the experimental conditions of the initially used stoichiometric mixture. The chloride anions from the copper salt seem able to deprotonate the ligand with subsequent formation of hydrochloric acid. Hence, copper chloride was replaced by copper acetate, primarily in order to increase the yield of this reaction, as well as a cautionary measure to avoid HCl build up [21]. The ligand HL^I (1 equiv.) was treated with $Cu(OAc)_2 \cdot 2H_2O$ (1 equiv.) in the presence of triethylamine as a base to support ligand deprotonation yielding the species $[Cu(L^I)OAc]$ (**2**) in 90% yield. The ESI(pos) MS spectrum shows the characteristic $m/z = 527.8$ associated with the fragment $[Cu(L^I)]^+$, whereas the acetate species was detected by infrared spectroscopy at 1586 and 1402 cm^{-1} as a monodentate ligand. Elemental analysis showed excellent agreement with the proposed formula.

The EPR spectra taken at 77 K for **1** and **2** reinforce this notion with values of $g_{\|} \approx 2.26, g_{\perp} \approx 2.06, A_{\|} \approx 174$ G and $A_{\perp} \approx 19$ G, thus typical of $3d^9$ copper(II) ions in nearly square planar environments [19d,f]. Furthermore, the UV–visible spectra of species **1** and **2** in methanol show the presence of a phenolate-to-copper charge transfer band at around 450 nm ($\varepsilon \approx 1250$ L/mol/cm) [19].

When a reaction of 2:1 stoichiometry between HL^I and the copper acetate salt was carried out in methanol, a green precipitate described

as [Cu(HL^{I})(L^{I})]OAc (**3**) was obtained. The compound was recrystallized in dichloromethane yielding a microcrystalline material. Although crystals suitable for X-ray diffraction were not obtained, infrared spectroscopy reveals the presence of acetate counterions, as displayed by prominent peaks at 1564 and 1439 cm^{-1}. Additional peaks at 3448 are attributed to the presence of OH stretches belonging to a protonated HL^{I} ligand. ESI mass spectra in the positive mode shows $m/z = 527.9$ characteristic of the [Cu(L^{I})]$^{+}$ fragment. In good agreement with the elemental analysis, these data confirm the presence of two ligands coordinated to copper, one of which remaining protonated. This coordination mode for copper has been observed in our laboratories with the analogous ligand HL^{tBu}, where tertiary butyl groups occupy the 2- and 4-positions of the phenol ring [20,22]. Species **3** shows EPR parameters $g_{\perp}$, $A_{\parallel}$, and $A_{\perp}$ similar to those of **1** and **2** but with $g_{\parallel} = 2.30$, thus, evidencing bonding along the *z*-axis typical of five-coordinate copper(II) ions [19d].

2.3. Molecular structure of *1*

Needle-like crystals of [Cu(L^{I})Cl] (**1**) were isolated and solved diffractometrically by means of X-ray diffraction. The crystal structure of **1** is shown in Fig. 2 and confirms its mononuclear nature. One copper(II) ion is coordinated to a deprotonated ligand with distances of 1.93 Å to the oxygen of the phenolate group, 1.99 Å to the amine nitrogen, and 2.02 Å for the pyridine nitrogen, resembling similar systems [19,22]. The coordination sphere is completed with the anionic chloro ligand occupying the fourth position 2.24 Å away from the metal. The copper center adopts a distorted square planar environment. One can, therefore, conclude that contrary to the tetradentate phenol-containing ligands described by Zurita [19f,23], tridentate ligands such as HL^{I} do not foster the formation of stable dimers in the solid state.

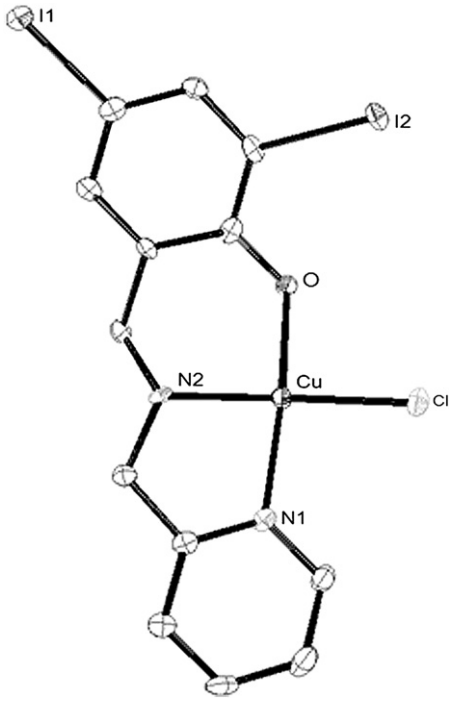

Fig. 2. ORTEP diagram at 50% probability level for [Cu(L^{I})Cl] (**1**) with selected bond lengths (Å) and angles (°). Cu(1)–O(1) = 1.929(3), Cu(1)–N(2) = 1.990(4), Cu(1)–N(1) = 2.018(4), Cu(1)–Cl(1) = 2.2488(14), N(2)–Cu(1)–Cl(1) = 162.63(14), O(1)–Cu(1)–N(1) = 66.40(17).

2.4. Antiproliferative effect of *1–3* in tumor cells

Our results thus far have allowed us to gain detailed understanding on the coordination chemistry of copper complexes as candidate drugs or prodrugs for cancer therapy. Human leukemia Jurkat T cells were treated with complexes **1–3** at different concentrations for 18 h, followed by trypan blue assay to assess cell death. This is a reliable assay that is reproducible and frequently used in our lab. All species tested demonstrated a dose-dependent increase in cell-killing activity with nearly 100% cell death at 15 μM, compared to a control treated with DMSO. The values given in Table 1 and Fig. 3 reflect the concentration at which each compound induces 50% cell death.

The 1:1 copper species **1** and **2** demonstrated IC_{50} values of 3.82 and 4.46 μmol/L. Interestingly, complex **3** exerted a similar degree of potency ($IC_{50} = 3.98$ μmol/L). Because the cation [Cu^{II}(L^{I})]$^{+}$ of **1** is isostructural with that of **2**, this observation suggests the 1:1 ligand-to-metal ratio as the possible pharmacophore and potential therapeutic agent. Furthermore, treatment of the cells with up to 50 μM of the ligand HL^{I} or the copper salt failed to induce death ratios greater than 10%. Due to the small standard deviation values between **1** and **2**, ascertaining the role played by the nature of the anionic ligand (chloride *vs.* acetate) remains unclear and further analysis will be necessary to provide a more conclusive result.

2.5. In vitro inhibition of proteasomal chymotryspin-like activity by *1–3*

In order to test the role of complexes **1–3** in targeting the cellular proteasome, we compared the independent activity of the salt $CuCl_2 \cdot 2H_2O$, the ligand HL^{I}, and that of a 1:1 mixture of copper chloride and the ligand HL^{I} toward C4-2B prostate cancer cell extract. The results indicate that both the copper chloride salt and the copper chloride:ligand mixture inhibit the chymotrypsin-like activity of the 26S proteasome with IC_{50} values of ~3.5 μM (Fig. 4a). In contrast, the ligand HL^{I} alone had a negligible effect, even at concentrations as high as 25 μM. This seems to be consistent with prior work in our laboratories in which the copper ion [14,15] is the driving force underlying proteasome inhibition. This suggests that the ligand is necessary as a carrier to preclude undesired nonspecific interactions of copper in the cell extract [23]. In order to underscore the role of the ligand, we tested complexes **1–3** under similar conditions. All species inhibited the proteasomal chymotrypsin-like activity in a concentration-dependent manner as shown in Fig. 4b.

2.6. Inhibition of chymotrypsin-like activity and induction of apoptosis by *1–3* in multiple prostate cancer cell lines

In the previous section we have discussed the inhibition of proteasomal chymotryspin-like activity under cell-free conditions. When intact prostate cancer cells were treated with HL^{I} or the Cu^{+2} ion at the 15 μmol/L concentration, less than 20% proteasome

Table 1
IC_{50} values for cell death induction by copper compounds. (a) Human leukemia Jurkat T cells were treated with copper compounds **1–3** for 18 h, followed by measurement of cell death in a trypan blue exclusion assay. Standard deviations are indicated.

Compound	Cell death induction IC_{50} μmol/L
1	3.82 ± 0.01
2	4.46 ± 0.01
3	3.98 ± 0.01
HL^{I}	No activity
$CuCl_2$	No activity

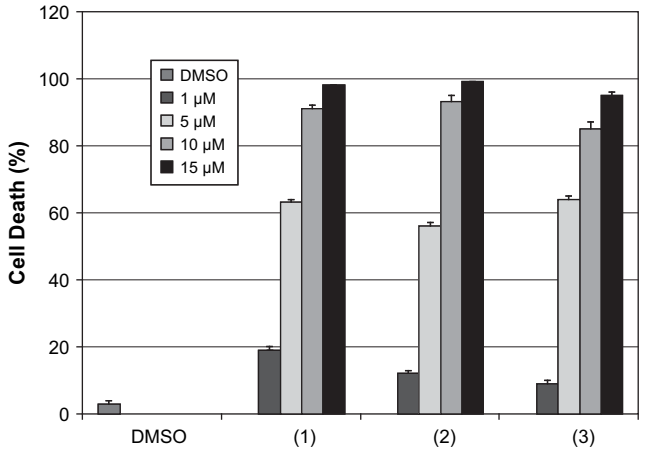

Fig. 3. IC_{50} values for cell death induction by **1**–**3**. (a) Human leukemia Jurkat T cells were treated with copper compounds **1**–**3** for 18 h, followed by measurement of cell death in a trypan blue exclusion assay. HLI, $CuCl_2$, and DMSO are used as controls. Standard deviations are shown as error bars.

inhibition was evident. In order to confirm the ability of the copper complexes to inhibit the proteasomal activity in cancer cells, two distinct prostate cell lines were tested, namely androgen receptor-positive C4-2B and androgen receptor-negative PC-3.

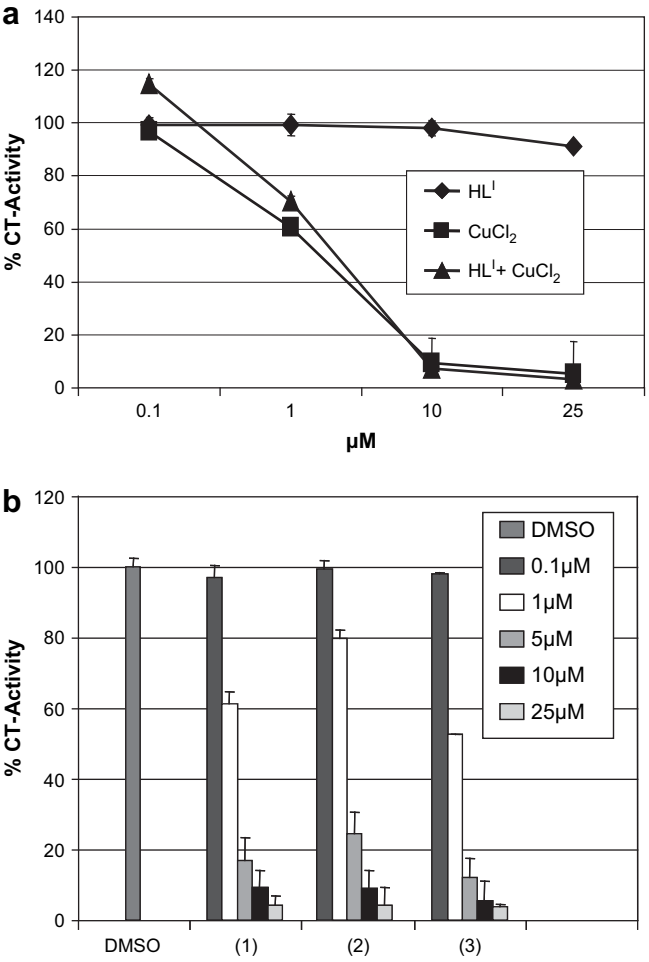

Fig. 4. *In vitro* proteasome-inhibitory activity of **1**–**3** in C4-2B cell extracts: (a) Proteasomal chymotrypsin-like activity (%CT) of the ligand HL^I, the salt $CuCl_2$, and an 1:1 HL^I:$CuCl_2$ mixture in DMSO at 25 mmol/L stock solution. (b) Concentration-dependent inhibition by **1**–**3** at 0.1, 1, 5, 10, and 25 μM.

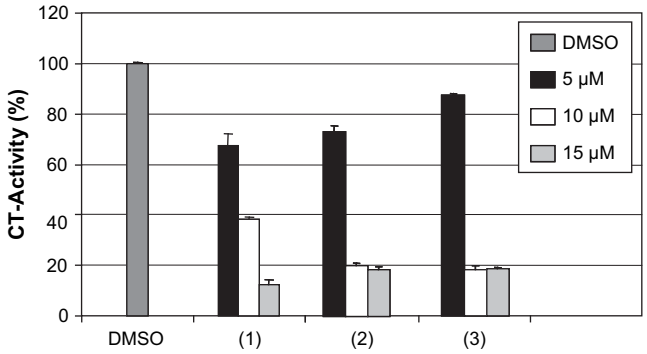

Fig. 5. Dose-dependent effects of **1**–**3** in C4-2B cells. The results were also compared to three negative controls (DMSO, HL^I, and $CuCl_2 \cdot 2H_2O$) for 18 h followed by measuring inhibition of proteasomal chymotrypsin-like activity.

The androgen receptor-positive C4-2B prostate cells: The cells were treated with compound **1** at 5, 10 and 15 μM concentrations for 18 h. The cells were harvested and proteins extracted, followed by measurement of proteasomal inhibition and apoptosis. Cells were also treated with the vehicle DMSO, the ligand HL^I, and the salt $CuCl_2 \cdot 2H_2O$ at the same concentrations to serve as negative controls. Compound **1** inhibits the proteasomal chymotrypsin-like activity in a dose-dependent manner by 35% at 5 μM, 62% at 10 μM and 85% at 15 μM (Fig. 5). Consistent with proteasome inhibition by **1**, levels of ubiquitinated proteins were also increased in a dose-dependent fashion in the treated C4-2B cells (Fig. 6). In a sharp contrast, cells treated with either the solvent, the ligand, or the copper salt failed to inhibit significantly the proteasome activity (Figs. 5 and 6 and data not shown). This fact provides strong evidence that the combination of copper(II) ion and ligand is a necessary requirement in order to cross the cellular membrane and reach the proteasome.

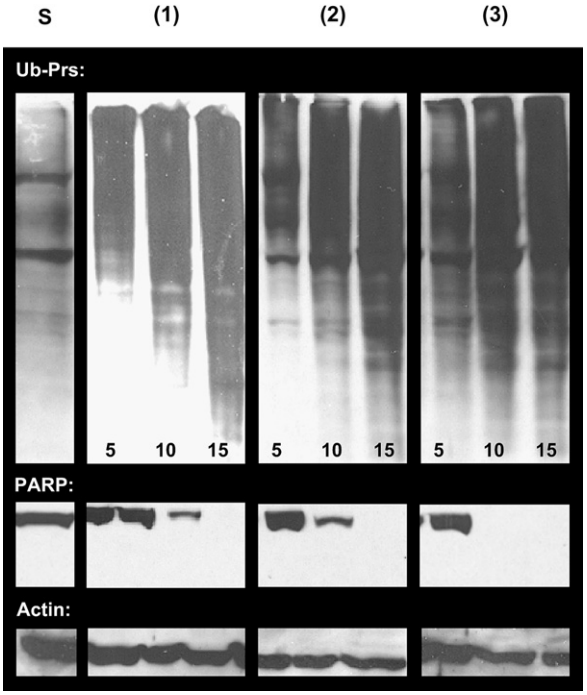

Fig. 6. Dose-dependent effects of **1**–**3** in C4-2B cells. Accumulation of ubiquitinated proteins (Ub-Prs), and cleavage of PARP.

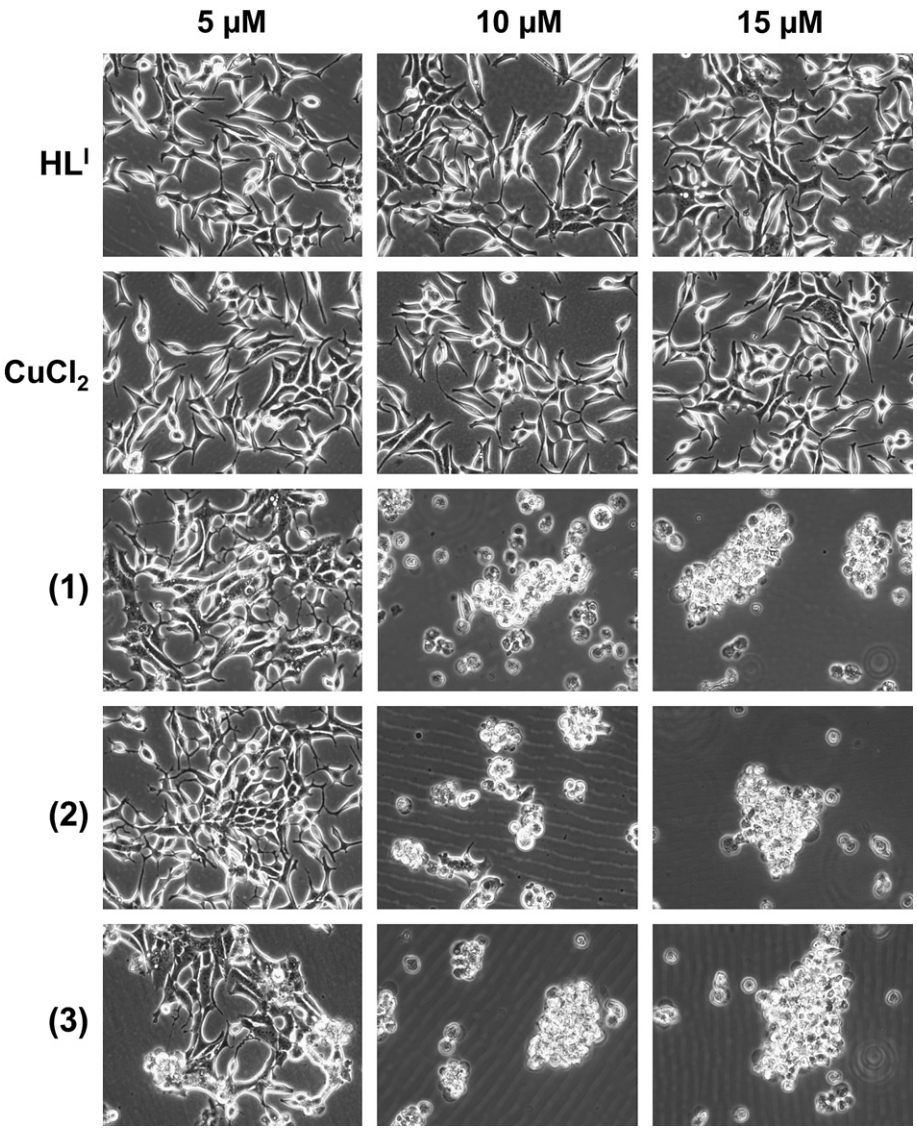

Fig. 7. Dose-dependent effects of **1**–**3** in C4-2B cells. Micrographs of apoptotic morphologic changes in HL^{I}, $CuCl_2$, **1**–**3** (low definition PNG file).

It has been shown that inhibition of the proteasomal chymotrypsin-like activity is associated with apoptosis of tumor cells [24]. To investigate whether the proteasomal inhibition by **1** is associated with apoptotic cell death, cleavage of the DNA repair protein, poly-(ADP-ribose) polymerase (PARP) and cellular morphological changes were measured in the same experiment. Cells showed a significant decrease in the levels of PARP protein (Fig. 5) when treated with **1** at 10 and 15 μM. Consistently, aberrant morphological changes, namely the rounded up shape and characteristic apoptotic blebbing shown in Fig. 6, were also observed in **1** in a concentration-dependent manner. Again, cells treated with DMSO, the ligand HL^{I}, or the salt $CuCl_2$ individually were unable to perturb the full length PARP fragment and no visible aberrant morphological changes were observed up to 15 μM tested (Figs. 6 and 7 and data not shown).

Similar results were also obtained from the C4-2B cells treated with compounds **2** and **3**: these two compounds inhibited about 80% of proteasomal activity at concentrations of 10 and 15 μM (Fig. 4), associated with increased levels of ubiquitinated proteins, decreased levels of PARP protein and the appearance of characteristic apoptotic cell morphology (Figs. 6 and 7).

These results show that the inhibition of proteasomal chymotrypsin-like activity in C4-2B cells is associated with the induction of apoptosis. Due to similar activity, it is also possible that in the 2:1 species **3**, the protonated ligand be labile and easily interchangeable suggesting that the active pharmacophore in both **2** and **3** is the cupric cation $[Cu(L^{I})]^{+}$.

The androgen receptor-negative PC-3 prostate cells: Upon demonstrating the ability of copper compounds to inhibit the proteasomal chymotrypsin-like activity in androgen receptor-positive C4-2B cells, we then tested the effect of compounds **2** and **3** on androgen receptor-negative PC-3 prostate cancer cells. PC-3 cells were treated respectively with different concentrations of **2** and **3**, copper salt, and HL^{I} for 18 h, followed by measurement of the proteasome activity, accumulated ubiquitinated proteins and apoptosis induction. We found that **3** could inhibit the chymotrypsin-like activity by ~30% and ~85% at 5 and 10 μmol/L, respectively, whereas **2** could inhibit the chymotrypsin-like activity by ~88% at 10 μmol/L (Fig. S1a). Additionally, cells treated with either $CuCl_2$ or HL^{I} showed no effect toward proteasome activity compared to the DMSO control.

Consistent with the inhibition of proteasomal chymotrypsin-like activity, significantly increased levels of ubiquitinated proteins

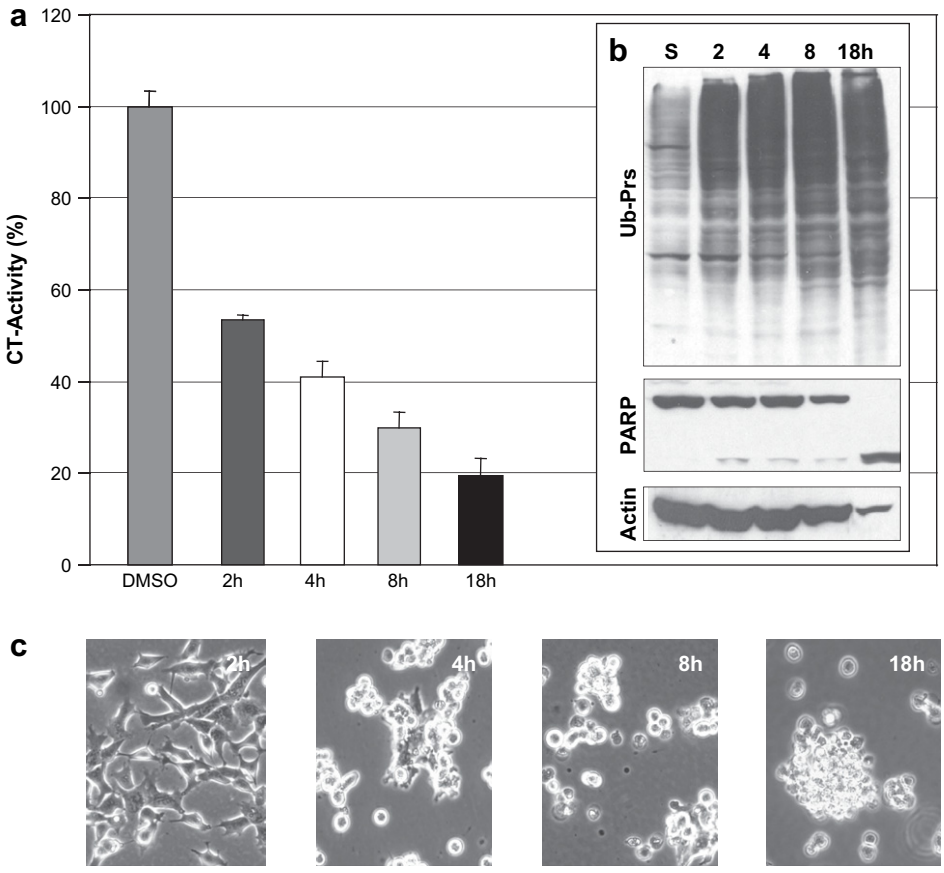

Fig. 8. Kinetic effect of proteasome inhibition and apoptosis induction by 2 in C4-2B cells. (a) Measurement of proteasomal chymotrypsin-like activity over time, (b) accumulated ubiquitinated proteins (UB-Prs) and PARP cleavage with actin as a loading control, and (c) apoptotic cellular morphological changes (low definition PNG file).

were detected in the PC-3 cells treated with **2** and **3** but not metal salt or HL^{I} (Fig. S1b). In the same experiment, treatment with **2** and **3** resulted in significant cellular detachment and cleavage of PARP, associated with apoptosis induction (Fig. S1c). These results show that as in C4-2B prostate cancer cells, copper compounds **2** and **3** could target and inhibit the proteasome in PC-3 cells. Our results remain consistent in that HL^{I} or the metal salt alone had little effect on proteasome activity and overall cellular integrity.

2.7. Kinetic effect of *1*–*3* on proteasome inhibition and apoptosis induction

The previous results show that complexes **1**–**3** demonstrated potent proteasome-inhibitory and apoptosis-inducing activities in multiple prostate cancer cell lines. In order to study the kinetic effect of copper complex-induced proteasome inhibition, C4-2B prostate cancer cells were treated with 15 μM of **2** for 2–18 h. The proteasomal chymotrypsin-like activity was inhibited by 45%, 60%, 70% and 80% after 2, 4, 8, and 18 h, respectively, as shown in the graph of Fig. 8a. The proteasomal chymotrypsin-like activity inhibition was associated with accumulated levels of ubiquitinated proteins (Fig. 7b). Additionally, higher levels of the proteasomal target p27 protein are visible at later time points (data not shown). Consistently, apoptosis-specific PARP cleavage was visible after 8 h treatment and full length PARP was completely cleaved into its respective p65 fragment after 18 h (Fig. 8b). This observation is also supported by abnormal morphological changes during later time points, as well as the appearance of rounded up and detached cells indicative of apoptosis, as shown by selected micrographs in Fig. 8c. These results clearly show that apoptosis induction occurs following inhibition of proteasomal activity. Therefore, proteasome inhibition appears to be a requirement for apoptosis induction.

2.8. Nontoxic effect of *1*–*3* in immortalized human breast cells

The ability to distinguish normal from malignant cells is imperative for developing successful anticancer drugs. To determine whether inhibition of proteasome activity achieved by copper compounds is selective toward malignant cells and not normal cells, we used normal immortalized human breast cell line, MCF-10A to test this effect. MCF-10A cells were treated with different concentrations of **2** and **3** up to 10 μmol/L for 18 h, followed by measurement of proteasomal chymotrypsin-like activity and apoptosis. We found that when these nontransformed cells were

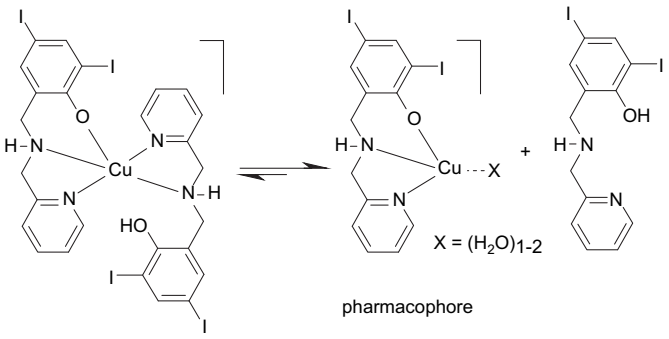

Scheme 2. Suggested conversion of **3** into a $[CuL^{I}(H_2O)_n]^{+}$ species.

Table 2
Crystal data and structure refinements for [Cu(L^I)Cl] (**1**).

Formula	$C_{13}H_{11}N_2O_1Cl_1I_2Cu_1$
FW	564.03
Space group	$P2_1/c$
a (Å)	6.8589(2)
b (Å)	16.9913(5)
c (Å)	27.0658(8)
β (°)	95.822(2)
V (Å^3)	3138.0(2)
Z	8
Temp (K)	100(2)
λ (Å)	0.71073
Density, calcd (g/cm^3)	2.388
μ (mm^{-1})	5.493
$R(F)$[a] (%)	4.12
$Rw(F)$[a] (%)	6.51

[a] $R(F) = \sum||\mathrm{Fo}| - |\mathrm{Fc}||\sum|\mathrm{Fo}|$; $Rw(F) = [\sum w(\mathrm{Fo}^2 - \mathrm{Fc}^2)^2/\sum w(\mathrm{Fo}^2)^2]^{1/2}$ for $I > 2\sigma(I)$.

treated with **2** and **3**, no proteasome inhibition was detected (Fig. S2a). Other treatments also had no or little effect on MCF-10A cells. To determine whether the inability of copper compounds to inhibit the proteasome activity is associated with the lack of apoptosis induction in these normal immortalized breast cells, apoptosis-associated morphological changes were then assessed in the same experiment. These normal, immortalized MCF-10A cells showed only little, if any, such cell death-related detachment after treatment with **2** and **3** up to 18 h (Fig. S2b). Our data suggest that these copper compounds could inhibit the proteasome activity and induce apoptosis selectively in human cancer cells but not in normal immortalized breast cells.

3. Conclusions

Following the encouraging results observed for similar gallium(III) complexes [18], this article presented the results of proteasome inhibition by copper(II) complexes of the iodo-substituted ligand HL^I as a potential anticancer therapeutic route. Three compounds with distinctive stoichiometries and nature of the anionic monodentate ligand were compared.

On one hand, it has been demonstrated that the non-metallated ligand is incapable of inhibiting the 20S proteasome activity. On the other hand, inhibition does occur by the copper(II) chloride salt, but only in cell-free conditions. Therefore, one could conclude that the primary function of the copper complexes is to serve as a carrier to cross the cell membrane. Once inside the cell, this complex is likely to cause proteasome inhibition by coordination of the metal center to available amino acids capable of forming Cu–N, Cu–S, or Cu–O bonds. If this hypothesis is correct, the stoichiometry of the complex is of paramount importance. Consistently, the 1:1 metal-to-ligand complexes **1** and **2** are comparable or slightly more effective than the 1:2 species **3**. Nonetheless, due to the small SD values in terms of cytotoxicity, it seems premature to make such a comparison. Copper(II), being a labile species, can gain stability by bonding to deprotonated and negatively charged phenolates and the nature of the anionic monodentate ligand *per se* may or may not be relevant. Species **1** and **2** have shown comparable proteasome-inhibitory activity *in vitro*. Therefore it can be suggested that the pharmacophore or active species could be described as $[CuLI]^+$. Due to stoichiometric constraints, equivalent solvated species such as $[CuLI(H_2O)]^+$ or $[CuLI(H_2O)_2]^+$ should also be considered. Granted that more detailed studies are necessary to provide final evidence, this pharmacophore would present an open coordination that facilitates interaction with available amino acids with high affinity for copper. It is viable that the active form of the copper complex binds to the amino-terminal threonine residue of the chymotryptic active center in the 20S proteasome. This hypothesis is based on known mechanisms for lactacystin, esters, epoxyketones, peptide derivatives, and boronates [8–13]. Recent data [25] indicating that the JAMM domain of the 19S caps in the 26S proteasome is another target for copper complexes suggest that further studies are necessary to assess this possibility and to ascertain the precise *locus* of coordination. It is also possible that **3** is a prodrug and in order to become active, the loss of a ligand must occur. This process would convert this compound into a similar $[CuL^I(H_2O)_n]^+$ species, as described in Scheme 2.

The depth of the therapeutic potential for metal-based proteasome inhibitors is yet to be determined. It is evident, however, that this can become a viable novel route to anticancer therapy. Ongoing work in our laboratories focus on (i) the metabolic stability and the pharmacokinetic behavior of these compounds, (ii) assessment of the role of anionic ligands, and (iii) on the inclusion of other bivalent metal centers such as cobalt, nickel, and zinc, and trivalent ions such as iron and ruthenium to assess the roles of ligand dissociation, the 1:1 and 1:2 metal-to-ligand stoichiometry, redox activity, and charge. We are also developing biomimetic models of the 1:1 gallium and copper species toward complexation with threonine and other amino acids and short peptides in order to determine the precise coordination loci within the proteasome.

4. Experimental section

4.1. Chemicals

All reagents were obtained from commercial sources. $CuCl_2 \cdot 2H_2O$ was purchased from Sigma–Aldrich (St. Louis, MO). Solvents were purified by means of an I.T. solvent purification system. RPMI 1640, penicillin and streptomycin were purchased from Invitrogen (Carlsbad, CA). Fetal bovine serum was purchased from Aleken Biologicals (Nash, TX). Fluorogenic peptide substrate Suc-LLVY-AMC (for the proteasomal chymotrypsin-like activity) were from Calbiochem (San Diego, CA). Mouse monoclonal antibody against human poly(AP-ribose) polymerase (PARP), p27, ubiquitin and secondary antibodies were from Santa Cruz Biotechnology, Inc. (Santa Cruz, CA).

4.2. Methods

ESI spectra were measured on a Micromass QuattroLC triple quadrupole mass spectrometer with an electrospray/APCI source and Walters Alliance 2695 LC, autosampler and photodiode array UV detector. Experimental assignments were simulated based on peak location and isotopic distributions. Infrared spectra were measured from 4000 to 400 cm^{-1} as KBr pellets on a Tensor 27 FTIR-spectrophotometer. UV–visible spectroscopy from 1.0×10^{-4} methanol or methanol:DMSO solutions was performed using a Cary 50 spectrometer in the range 250–1000 nm. The samples were mortar-ground and heat-dried under vacuum overnight to eliminate solvent molecules. First derivative X-Band EPR spectra of 1.0×10^{-3} M methanol solutions were performed with a Bruker ESP 300 spectrometer using liquid helium as the coolant. Elemental analyses were performed by Midwest Microlab, Indianapolis, IN. Cellular morphology analyses and imaging with phase contrast were performed on a Zeiss Axiovert 25 microscope.

4.2.1. X-ray structural determination for [Cu(L^I)(Cl)] (**1**)

Diffraction data were measured at 100 K on a Bruker *X8 APEX-II* kappa geometry diffractometer with Mo radiation and a graphite monochromator. Frames were collected as a series of sweeps with the detector at 40 mm and 0.3° between each frame, recorded for 10 or 20 s. *APEX-II* [26] and *SHELX-97* [27] software were used in the

collection and refinement (Table 2). Crystals of **1** [$C_{13}H_{11}N_2O_1Cl_1I_2Cu_1$] were blue-green needles; the diffraction sample was $0.4 \times 0.02 \times 0.01$ mm^3. 50 251 total reflections were recorded, yielding 7828 independent *hkl* data. Hydrogen atoms were placed in calculated positions. The asymmetric unit consists of two independent neutral complexes.

4.3. Syntheses

The ligand 2,4-diiodo-6-((pyridine-2-ylmethylamino) methyl)-phenol was synthesized according to a previously published procedure [16].

4.3.1. [Cu(L^I)Cl] (**1**)

0.50 g, 1.1 mmol of HL^I was dissolved in 15 mL of DMSO. After 5 min, 0.18 g, 1.2 mmol of $CuCl_2 \cdot 2H_2O$ was dissolved in 15 mL of DMSO and the resulting solution was added dropwise and stirred at room temperature for 45 min. The green solution was added to 15 mL of cold ethanol to afford dark green needle-like crystals after 48 h. Yield = 0.15 g (27%). Elemental analysis calc. (%) for $C_{13}H_{11}ClCuI_2N_2O$: C 27.68; H 1.97; N 4.97. Found: C, 27.72; H, 1.88; N, 4.86. IR data (KBr, cm^{-1}): 3073 ν(N–H); ESI$^+$ MS data (MeOH): m/z = 527.9 for [CuL]$^+$, 605.9 [CuL–DMSO]$^+$.

4.3.2. [Cu(L^I)OAc] (**2**)

0.50 g, 1.1 mmol of HL^I was dissolved in 15 mL of DMSO and treated with 1.1 equiv. of triethylamine. While stirring for 5 min at room temperature, 0.27 g, 1.2 mmol of $Cu(OAc)_2 \cdot 2H_2O$ was dissolved in 15 mL of DMSO and the ligand solution was added dropwise and allowed to react for 45 min. The complex was isolated using suction filtration and washed with cold methanol and ether to afford a green precipitate. Yield = 0.505 g (86%). Elemental analysis calc. (%) for $C_{15}H_{14}CuI_2N_2O_3$: C 30.66; H 2.40; N 4.77. Found: C, 30.82; H, 2.45; N, 4.70. IR data (KBr, cm^{-1}): 3073 ν(N–H); 1586 ν_{asym}(OAc$^-$); 1402 ν_{sym}(OAc$^-$). ESI$^+$ MS data (MeOH): m/z = 527.8 for [CuL]$^+$, 606.0 [CuL–DMSO]$^+$.

4.3.3. [Cu(HL^I)(L^I)]OAc (**3**)

A 15 mL methanol solution of HL^I (1.05 g, 2.1 mmol) was added dropwise to a 15 mL methanol solution of $Cu(OAc)_2 \cdot 2H_2O$ (0.27 g, 1.2 mmol) at 45 °C. After 45 min a green precipitate was obtained, isolated by frit filtration, and washed with cold methanol and ether. The solid was recrystallized in dichloromethane. Yield = 0.900 g (79%). Elemental analysis calc (%) for **3** CH_2Cl_2 $C_{29}H_{28}Cl_2CuI_4N_4O_4$: C 30.59; H 2.48; N 4.92. Found: C, 30.82; H, 2.42; N, 4.76. IR data (KBr, cm^{-1}) 3448 ν(OH); 3076 ν(N–H); 1564 ν_{asym}(OAc$^-$); 1439 ν_{sym}(OAc$^-$). ESI$^+$ MS data (MeOH): m/z = 527.9 for [CuL]$^+$, 994 (minor) for [Cu(HL)(L)]$^+$.

4.4. Trypan blue assay

The trypan blue dye exclusion assay was performed by mixing 100 μL of cell suspension with 50 μL of 0.4% trypan glue dye before injecting into a hemocytometer and counting. The number of cells that absorbed the dye and those that excluded the dye were counted, from which the percentage of nonviable cell number to total cell number was calculated.

4.5. Cell cultures and whole-cell extract preparation

Human prostate cancer cells C4-2B and PC-3 were grown in RPMI 1640 medium supplemented with 10% FBS and maintained at 37 °C and 5% CO_2. MCF-10A cells (normal, derived from benign human breast tissue) were obtained and cultured as previously described. A whole-cell extract was prepared [14b].

4.6. Analysis of the proteasomal activity in whole-cell extract

C4-2B, PC-3 and MCF-10A whole-cell extract (8 μg) was incubated with 10 μmol/L chymotrypsin-like substrate (Suc-LLVY-AMC) in 100 μL assay buffer [50 mmol/L Tris–HCl (pH 7.5)] in the presence of different copper compounds, ligand, and inorganic copper salt at various concentrations or solvent DMSO as control. After a 2 h incubation at 37 °C, production of hydrolyzed AMC groups was measured using a Wallac Victor3™ multilabel counter with an excitation filter of 365 nm and an emission filter of 460 nm [14b].

4.7. Western blot analysis

Cell extracts were separated by SDS-PAGE and transferred to a nitrocellulose membrane. Western blot analysis was performed using specific antibodies to p27, ubiquitin, or PARP (Santa Cruz Biotechnology Inc, Santa Cruz, CA) followed by visualization using the HyGLO reagent (Denville Scientific, Metuchen, NJ).

Acknowledgements

S.S.H. and M.F. contributed equally to this publication. C.N.V. gratefully acknowledges the Wayne State University and partial support from the National Science Foundation (CHE-0718470). Q.P.D. acknowledges the Karmanos Cancer Institute of Wayne State University, the Department of Defense Breast Cancer Research Program (W81XWH-04-1-0688 and DAMD17-03-1-0175) and the National Cancer Institute (1R01CA120009). M.F. acknowledges a training grant, "Ruth L. Kirschstein National Service Research Award" (T32-CA009531).

Appendix. Supporting information

Supplementary data associated with this article can be found in the online version, at doi:10.1016/j.ejmech.2009.05.019.

References

[1] L. Kelland, Nat. Rev. Cancer 7 (2007) 573.
[2] (a) M. Pavelka, M.F.A. Lucas, N. Russo, Chem. Eur. J. 13 (2007) 10108;
(b) R.C. Todd, K.S. Lovejoy, S.J. Lippard, J. Am. Chem. Soc. 129 (2007) 6370;
(c) V. Beljanski, J.M. Villanueva, P.W. Doetsch, G. Natile, L.G. Marzilli, J. Am. Chem. Soc. 127 (2005) 15833;
(d) M.A. Fuertes, C. Alonso, J.M. Pérez, Chem. Rev. 103 (2003) 645;
(e) D.V. Deubel, J. Am. Chem. Soc. 124 (2002) 5834;
(f) E.R. Jamieson, S.J. Lippard, Chem. Rev. 99 (1999) 2467.
[3] (a) C.X. Zhang, S.J. Lippard, Curr. Opin. Chem. Biol. 7 (2003) 481;
(b) L.R. Kelland, N. Farrell, Platinum-based Drugs in Cancer Therapy, Humana Press, Totowa, 2000.
[4] (a) M.A. Jakupec, M. Galanski, V.B. Arion, C.G. Hartinger, B.K. Keppler, Dalton Trans. (2008) 183;
(b) S.P. Fricker, Dalton Trans. 43 (2007) 4903;
(c) D.S. Kalinowski, P.C. Sharpe, P.V. Bernhardt, D.R. Richardson, J. Med. Chem. 50 (2007) 6212;
(d) S. Tardito, O. Bussolati, M. Maffini, M. Tegoni, M. Giannetto, V. Dall'Asta, R. Franchi-Gazzola, M. Lanfranchi, M.A. Pellinghelli, C. Mucchino, G. Mori, L. Marchio, J. Med. Chem. 50 (2007) 1916;
(e) U. Schatzschneider, N. Metzler-Nolte, Angew. Chem., Int. Ed. 45 (2006) 1504.
[5] (a) A.L. Goldberg, Biochem. Soc. Trans. 35 (2007) 12;
(b) A.L. Goldberg, Science 268 (1995) 522;
(c) L. Borissenko, M. Groll, Chem. Rev. 107 (2007) 687–717.
[6] Q.P. Dou, B. Li, Drug Resist. Updat. 2 (1999) 215.
[7] S.V. Rajkumar, P.G. Richardson, T. Hideshima, K.C. Anderson, J. Clin. Oncol. 23 (2005) 630.
[8] C.E. Masse, A.J. Morgan, J. Adams, J.S. Panek, Eur. J. Org. Chem. 14 (2000) 2513.
[9] (a) N. Basse, S. Piguel, D. Papapostolou, A. Ferrier-Berthelot, N. Richy, M. Pagano, P. Sarthou, J. Sobczak-Thepot, M. Reboud-Ravaux, J. Vidal, J. Med. Chem. 50 (2007) 2842;
(b) M. Groll, M. Goetz, M. Kaiser, E. Weyher, L. Moroder, Chem. Biol. 13 (2006) 607;
(c) Y. Koguchi, J. Kohno, M. Nishio, K. Takahashi, T. Okuda, T. Ohnuki, S. Komatsubara, J. Antibiot. 53 (2000) 105.

[10] (a) M. Groll, K.B. Kim, N. Kairies, R. Huber, C.M. Crews, J. Am. Chem. Soc. 122 (2000) 1237;
(b) M. Elofsson, U. Splittgerber, J. Myung, R. Mohan, C.M. Crews, Chem. Biol. 6 (1999) 811.
[11] (a) E.S. Lightcap, T.A. McCormack, C.S. Pien, V. Chau, J. Adams, P. Elliott, Clin. Chem. 46 (2000) 673;
(b) G. Loidi, M. Groll, H.J. Musiol, R. Huber, L. Moroder, Proc. Natl. Acad. Sci. U.S.A. 96 (1999) 5418;
(c) R.T. Lum, M.G. Nelson, A. Joly, A.G. Horsma, G. Lee, S.M. Meyer, M.M. Wick, S.R. Schow, Bioorg. Med. Chem. Lett. 8 (1998) 209;
(d) J.F. Lynas, P. Harriott, A. Healy, M.A. Mckarvey, B. Walker, Bioorg. Med. Chem. Lett. 8 (1998) 373;
(e) A. Vinitsky, C. Cardozo, L. Sepp-Lorenzio, C. Machaud, M. Orlowski, J. Biol. Chem. 269 (1994) 29860.
[12] (a) J. Labutti, I. Parsons, R. Huang, G. Miwa, L.-S. Gan, J.S. Daniels, Chem. Res. Toxicol. 19 (2006) 539;
(b) M. Vivier, A.-S. Jarrousse, B. Bouchon, M.-J. Galmier, P. Auzeloux, J. Sauzieres, J.-C. Madelmont, J. Med. Chem. 48 (2005) 6731;
(c) T. Hideshima, C. Mitsiades, M. Akiyama, T. Hayashi, D. Chauhan, P. Richardson, R. Schlossman, K. Podar, N.C. Munshi, N. Mitsiades, K.C. Anderson, Blood 101 (2003) 1530;
(d) J. Adams, V.J. Palombella, E.A. Sausville, J. Johnson, A. Destree, D.D. Lazarus, J. Maas, C.S. Pien, S. Prakash, P.J. Elliott, Cancer Res. 59 (1999) 2615.
[13] M. Groll, C.R. Berkers, H.L. Ploegh, H. Ovaa, Structure 14 (2006) 451.
[14] (a) K.G. Daniel, P. Gupta, R.H. Harbach, C. Guida, Q.P. Dou, Biochem. Pharmacol. 67 (2004) 1139;
(b) K.G. Daniel, D. Chen, S. Orlu, Q.C. Cui, F.R. Miller, Q.P. Dou, Breast Cancer Res. 7 (2005) R897.
[15] D. Chen, Q.P. Dou, Expert Opin. Ther. Targets 12 (2008) 739.
[16] (a) R. Shakya, F. Peng, J. Liu, M.J. Heeg, C.N. Verani, Inorg. Chem. 45 (2006) 6263;
(b) R. Shakya, C. Imbert, H.P. Hratchian, M. Lanznaster, M.J. Heeg, B.R. McGarvey, M.M. Allard, H.B. Schlegel, C.N. Verani, Dalton Trans. (2006) 2517–2525.
[17] M. Frezza, C.N. Verani, D. Chen, Q.P. Dou, Lett. Drug Des. Discov. 4 (2007) 311.
[18] D. Chen, M. Frezza, R. Shakya, C.Q. Cui, V. Milacic, C.N. Verani, Q.P. Dou, Cancer Res. 67 (2007) 9258.
[19] (a) F. Michel, F. Thomas, S. Hamman, C. Philouze, E. Saint-Aman, J.-L. Pierre, Eur. J. Inorg. Chem. I-18 (2006) 3684–3696.(b) Y. Shimazaki, S. Huth, A. Odani, O. Yamauchi, Angew. Chem. 112 (2000) 1732;
Angew. Chem., Int. Ed. 39 (2000) 1666;
(c) S. Itoh, M. Taki, S. Takayama, S. Nagatomo, T. Kitagawa, N. Sakurada, R. Arakawa, S. Fukuzumi, Angew. Chem., Int. Ed. 38 (1999) 2774;
(d) A. Neves, C.N. Verani, M.A. de Brito, I. Vencato, A. Mangrich, G. Oliva, D.D.H.F. Souza, A.A. Batista, Inorg. Chim. Acta 290 (1999) 207;
(e) M. Vaidyanathan, R. Viswanathan, M. Palaniandavar, T. Balasubramanian, P. Prabhaharan, T.P. Muthiah, Inorg. Chem. 37 (1998) 6418;
(f) D. Zurita, I. Gautier-Luneau, S. Ménage, J.-L. Pierre, E. Saint-Aman, J. Biol. Inorg. Chem. 2 (1997) 46.
[20] S.S. Hindo, Synthesis, Structure, Electrochemistry, Spectroscopy, and Reactivity of Phenolate-Based Copper(II) Archetypes and Modules for Magnetic Soft Materials. M.Sc. Dissertation, Wayne State University, Detroit, MI, 2005.
[21] (a) C.J. Kim, S.J. Lee, M.H. Seo, N.Y. Cho, U.D. Sohn, M.Y. Lee, Y.K. Shin, S.S. Sim, Arch. Pharm. Res. 25 (2002) 675;
(b) S.B. Olaleye, E.O. Farombi, Phytother. Res. 20 (2006) 14.
[22] F.D. Lesh, S.S. Hindo, M.J. Heeg, M.M. Allard, P. Jain, B. Peng, L. Hryhorczuk, C.N. Verani, Eur. J. Inorg. Chem. (2009) 345.
[23] G.J. Brewer, Exp. Biol. Med 232 (2007) 323.
[24] U.G. Lopes, P. Erhardt, R. Yao, G.M. Cooper, J. Biol. Chem. 272 (1997) 12893.
[25] B. Cvek, V. Milacic, J. Taraba, Q.P. Dou, J. Med. Chem. 51 (2008) 6256–6258.
[26] SMART and APEX II Collection and Processing Programs are Distributed by the Manufacturer, Bruker AXS Inc., Madison, WI, USA.
[27] G. Sheldrick, SHELX-97, University of Gottingen, Germany, 1997.